Original article

MOLECULAR METABOLISM

Adipose tissue glycogen accumulation is associated with obesity-linked inflammation in humans

Victòria Ceperuelo-Mallafré [1,2,11], Miriam Ejarque [1,2,11], Carolina Serena [1,2], Xavier Duran [2], Marta Montori-Grau [2,3], Miguel Angel Rodríguez [2,4], Oscar Yanes [2,5], Catalina Núñez-Roa [1,2], Kelly Roche [1,2], Prasanth Puthanveetil [6], Lourdes Garrido-Sánchez [7,8], Enrique Saez [9], Francisco J. Tinahones [7,8], Pablo M. Garcia-Roves [10], Anna Mª Gómez-Foix [2,3,†], Alan R. Saltiel [6], Joan Vendrell [1,2,*,12], Sonia Fernández-Veledo [1,2,*,12]

ABSTRACT

Objective: Glycogen metabolism has emerged as a mediator in the control of energy homeostasis and studies in murine models reveal that adipose tissue might contain glycogen stores. Here we investigated the physio(patho)logical role of glycogen in human adipose tissue in the context of obesity and insulin resistance.

Methods: We studied glucose metabolic flux of hypoxic human adipoctyes by nuclear magnetic resonance and mass spectrometry-based metabolic approaches. Glycogen synthesis and glycogen content in response to hypoxia was analyzed in human adipocytes and macrophages. To explore the metabolic effects of enforced glycogen deposition in adipocytes and macrophages, we overexpressed PTG, the only glycogen-associated regulatory subunit (PP1-GTS) reported in murine adipocytes. Adipose tissue gene expression analysis was performed on wild type and homozygous PTG KO male mice. Finally, glycogen metabolism gene expression and glycogen accumulation was analyzed in adipose tissue, mature adipocytes and resident macrophages from lean and obese subjects with different degrees of insulin resistance in 2 independent cohorts.

Results: We show that hypoxia modulates glucose metabolic flux in human adipocytes and macrophages and promotes glycogenesis. Enforced glycogen deposition by overexpression of PTG re-orients adipocyte secretion to a pro-inflammatory response linked to insulin resistance and monocyte/lymphocyte migration. Furthermore, glycogen accumulation is associated with inhibition of mTORC1 signaling and increased basal autophagy flux, correlating with greater leptin release in glycogen-loaded adipocytes. PTG-KO mice have reduced expression of key inflammatory genes in adipose tissue and PTG overexpression in M0 macrophages induces a pro-inflammatory and glycolytic M1 phenotype. Increased glycogen synthase expression correlates with glycogen deposition in subcutaneous adipose tissue of obese patients. Glycogen content in subcutaneous mature adipocytes is associated with BMI and leptin expression.

Conclusion: Our data establish glycogen mishandling in adipose tissue as a potential key feature of inflammatory-related metabolic stress in human obesity.

Keywords Glycogen; Adipocyte; Macrophage; Autophagy; Obesity; Insulin resistance

[1]Hospital Universitari de Tarragona Joan XXIII, Institut d'Investigació Sanitària Pere Virgili, Universitat Rovira i Virgili, Tarragona, Spain [2]CIBER de Diabetes y Enfermedades Metabólicas Asociadas (CIBERDEM), Instituto de Salud Carlos III, Madrid, Spain [3]Departament de Bioquímica i Biologia Molecular, Institut de Biomedicina de la Universitat de Barcelona (IBUB), Facultat de Biologia, Universitat de Barcelona, Barcelona, Spain [4]Centre for Omic Sciences (COS), Institut d'Investigació Sanitària Pere Virgili, Universitat Rovira i Virgili, Tarragona, Spain [5]Department of Electronic Engineering, Universitat Rovira i Virgili, Tarragona, Spain [6]Life Sciences Institute, University of Michigan, Ann Arbor, MI, USA [7]Hospital Universitario Virgen de la Victoria, Instituto de Investigaciones Biomédicas de Málaga (IBIMA), Universidad de Málaga, IBIMA, Spain [8]CIBER de Fisiopatología de Obesidad y Nutrición (CIBEROBN), Instituto de Salud Carlos III, Madrid, Spain [9]Department of Chemical Physiology and The Skaggs Institute for Chemical Biology, The Scripps Research Institute, La Jolla, CA, USA [10]Departamento de Ciencias Fisiológicas II, Facultad de Medicina, Universitat de Barcelona, Barcelona, Spain

[11] Co-first authors.
[12] Co-senior authors.
[†] Deceased.

*Corresponding authors. Research Unit, University Hospital of Tarragona Joan XXIII, c/o Dr. Mallafré Guasch, 4, 43007 Tarragona. Spain. Tel.: +34 977 29 58 00; fax: +34 977 29 58 23. E-mails: jvortega2002@gmail.com (J. Vendrell), sonia.fernandezveledo@gmail.com (S. Fernández-Veledo).

Received September 17, 2015 • Revision received October 2, 2015 • Accepted October 9, 2015 • Available online 16 October 2015

http://dx.doi.org/10.1016/j.molmet.2015.10.001

1. INTRODUCTION

Adipose tissue is a highly complex metabolic organ with essential roles in handling and storing excess nutrients and preventing ectopic lipid accumulation in other organs. Excess lipid storage in adipose tissue leads to changes in its metabolic and endocrine functions, resulting in the generation of stress signals and the derangement of carbohydrate metabolism, among others [1]. In this setting, not only adipocytes but also infiltrating adipose tissue macrophages (ATMs), among other immune cells, participate in the chronic low-grade inflammation that occurs in the adipose tissue of obese individuals [2].

While triglyceride stored in adipose tissue is considered the principal energy reserve in mammals, glucose can also be stored as glycogen, primarily in liver and skeletal muscle, for mobilization during times of energy deficit. In humans, hepatic and skeletal muscle glycogen deposition is decreased under pathologic conditions associated with obesity, such as insulin resistance and type 2 diabetes [3–7], and is a hallmark of metabolic stress.

Glycogen synthesis is dynamically regulated by insulin through coordinated dephosphorylation of the key glycogenic enzyme glycogen synthase (GS) by the serine/threonine phosphatase PP1, which results in its activation, and the glycogenolytic enzyme glycogen phosphorylase (GP), which is inactivated [8]. The PP1 catalytic subunit (PP1c) is targeted to glycogen particles by glycogen-associated targeting subunits (PP1-GTS), including PPP1R3A (G_M, R_{GL}), PPP1R3B (G_L), PPP1R3C (PTG, or protein targeting to glycogen), PPP1R3D (PPP1R6) and PPP1R3E. PP1-GTS exhibit tissue and species-specific expression and play critical roles in the hormonal regulation of cellular glycogen metabolism [9–11].

Although present in low quantities, studies in murine models have shown that adipose tissue can store glycogen [12,13]. *Pp1r3c* was identified in a two-hybrid screen of a 3T3–L1 adipocyte library [14] and, to date, remains the only reported PP1-GTS expressed in murine adipocytes. Transgenic overexpression of PTG in adipose tissue increases glucose flux into the glycogen synthesis pathway, indicating that adipocytes are capable of storing high levels of glycogen. Interestingly, although adipocyte function appeared to be maintained in these animals, leptin, but not adiponectin, protein content in adipose tissue was increased, and the associated hyperleptinemia was independent of fat mass [15]. Further studies showed that upon caloric excess-induced expansion of adipose tissue mass, the elevated levels of glycogen in this model inhibited the mobilization of triglyceride and impeded weight loss following the return to chow feeding [16].

There is a paucity of research on the potential physio(patho)logical role of glycogen metabolism in adipose tissue. We hypothesized that obesity redirects glucose metabolic flux into glycogen synthesis in human adipocytes. Here we show that hypoxia, which has been linked to obesity-related adipose tissue dysfunction, increases glucose uptake and stimulates glycogen synthesis in adipocytes. Glycogen-loaded adipocytes exhibit increased autophagic flux, which directly impacts their endocrine secretory function. Furthermore, enforced glycogen deposition by overexpression of PTG in macrophages promotes polarization towards the M1 pro-inflammatory phenotype. Studies with human clinical samples confirm the interplay between autophagy and glycogen storage and show that human obesity is associated with glycogen deposition in adipocytes. Overall, our data demonstrate that glycogen accumulation in adipocytes and macrophages contributes to adipose tissue inflammation, and might underlie the metabolic alterations in obesity.

2. METHODS

2.1. In vitro cell cultures

The SGBS cell line, provided by Dr. Wabitsch (University of Ulm, Germany) and Lisa-2 cells, provided by Dr. Möller (University of Ulm, Germany), were used as cellular models of human subcutaneous and visceral pre-adipocytes, respectively, and were induced to differentiate as described [17]. THP-1 cells (a human monocytic cell line; ATCC, Rockville, MD) were induced to differentiate to macrophages with PMA as previously described [18]. The human myogenic cell line LHCN-M2 was used as a cellular model of human myoblasts. For migration experiments, monocytic THP-1 cells and Jurkat cells (human *T cell* lymphoblast-like *cell* line; ATCC, Rockville, MD) were grown in suspension. hASCs were isolated from the adipose tissue of lean patients (BMI 22.5 $\pm$ 0.3) following published protocols [19]. For hypoxia experiments, fully differentiated cells were cultured in a modular incubator flushed with 2% O_2, 93% N_2, and 5% CO_2. As controls, cells were cultured in a standard incubator (21% O_2 and 5% CO_2). Human adipose tissue-derived macrophages were isolated from the stromal-vascular fraction as previously described [20].

2.2. Adenoviral transduction

Cells were infected 7 days after induction of differentiation with an adenovirus expressing murine PTG (Ad-PTG) [21] or GFP (Ad-GFP) under the control of the CMV promoter [10]. Adenoviral infection was carried out for 2 h at a multiplicity of infection (moi) of 50. One day after infection, culture medium was depleted of insulin and FBS and metabolic experiments were performed 24 h later.

2.3. Gene expression analysis

Total RNA was extracted from adipose tissue/cells using the RNeasy Lipid Tissue Midi Kit (Qiagen Science, Hilden, Germany). Total RNA quantity was measured at 260 nm and purity was assessed by the OD260/OD280 ratio. One microgram of RNA was reverse transcribed with random primers using the Reverse Transcription System (Applied Byosistems, Foster City, CA). Quantitative gene expression was evaluated by Real-time PCR (qPCR) on a 7900HT Fast Real-Time PCR System using TaqMan® Gene Expression Assays (Applied Biosystems) for *in vitro* experiments and TaqMan® Low Density Arrays (Applied Biosystems, microfluidic cards) for studies with human samples (See Supplementary Experimental Procedures for all evaluated genes). Results were calculated using the comparative Ct method (2-$\Delta\Delta$Ct), and expressed relative to the expression of the housekeeping genes cyclophilin 1A (*PPIA*) (Hs 04194521_s1) and 18S (Hs 03928985_g1).

2.4. Glycogen synthesis rate

Cells were incubated with 20 mM [U-14C]glucose (0.05 μCi/μmol). To extract glycogen, cell monolayers were scraped into 100 μl of 30% (w/v) KOH and homogenates were boiled for 15 min. Homogenates were spotted onto Whatman 3 MM paper, and glycogen was precipitated by immersing the paper in ice-cold 66% (v/v) ethanol. Radioactivity in dried papers was counted in a beta-radiation counter. Glycogen synthesis rate was calculated as nanomoles of glucose incorporated per milligram of protein, and results were expressed as the percentage of stimulation over basal (control = 100) [10].

2.5. Glycogen content determination

Cell monolayers were scraped in 30% (wt/vol.) KOH. Homogenates were spotted onto Whatman 3 MM paper, and glycogen was precipitated in ice-cold 66% (vol./vol.) ethanol. The papers were incubated in

0.4 mol/l acetate buffer, pH 4.8, with 0.833 mg/ml α-amyloglucosidase (Sigma—Aldrich, St. Louis, MO) for 120 min at 37 °C. Glucose release was measured with a glucose kit from Biosystems SA (Barcelona, Spain). Glycogen was also visualized in duplicate paraffin-embedded tissue sections by the periodic acid/salicyloyl hydrazide (PA-SH) method [22]. Half of the samples were incubated with alpha-amylase (Sigma—Aldrich, St. Louis, MO) for 10 min at 30 °C as a negative control. Other sections were stained with standard hematoxylin for histological examination.

2.6. Immunofluorescence detection of glycogen

Adipocytes grown on coverslips were fixed with 4% (w/v) paraformaldehyde, rehydrated with 2% (v/v) fish skin gelatin, and permeabilized with 0.2% Triton X-100 prior to incubation with 5% (v/v) goat serum. Subsequently, cells were incubated overnight at 4 °C with a monoclonal mouse anti-glycogen antibody in PBS containing 1% goat serum. Coverslips were washed with PBS and incubated for 1 h at room temperature with 1:100 Alexa Fluor 568 conjugated goat anti-mouse followed by mounting with Pro Long Gold Antifade Reagent with 4′,6-diamidino-2-phenylindole, DAPI (Invitrogen Inc., Eugene OR). Microscopy was performed with a Leica DM 4000B fluorescence microscope (Leica Microsystems, Wetzlar, Germany) and images were captured with a Leica DFC 300 FX camera (Leica Microsystems). For glycogen staining in human adipose tissue, freshly isolated fat depots were fixed in 10% formalin and embedded in paraffin. Tissue sections (5 μm) were deparaffinized and rehydrated, and immunofluorescence detection of glycogen was performed as described above.

2.7. Transmission electron microscopy

Small human subcutaneous adipose tissue fragments (3 mm^2) were fixed with 2.5% paraformaldehyde, 1.5% glutaraldehyde in 0.1 M phosphate buffer (pH 7.2) for 3—6 h at 4 °C. Samples were then washed for 3—12 h with the same buffer and postfixed with 1% osmium tetroxide in the same buffer at 4 °C for 1 h. Samples were washed in water for 3—12 h and dehydrated in acetone, infiltrated with Epon (Epon 812) resin for 2 days at room temperature, embedded in the same resin and polymerized at 60 °C for 48 h. Ultrathin sections were obtained using a Leica (MZ6) Ultracut UCT ultramicrotome and mounted on Formvar-coated copper grids. Sections were stained with 2% uranyl acetate in water and lead citrate. Then, sections were examined and photographed using a JEM-1010 electron microscope (Jeol, Japan).

2.8. Immunoblot analysis

Cells and human biopsies were lysed and homogenized in RIPA buffer containing Protease Inhibitor Cocktail (Sigma—Aldrich), and protein concentration was determined with the BCA Protein Assay Kit (Pierce Biotechnology, Boston, MA). Equal amounts of total protein were separated on SDS-PAGE gels, transferred to Immobilon membranes and blocked [23]. Immunoreactive bands were visualized with SuperSignal West Femto chemiluminescent substrate (Pierce) and images were captured using the VersaDoc imaging system and Quantity One software (Bio-Rad, Hercules, CA).

2.9. Study selection and sample processing

Subjects were recruited by the Endocrinology and Surgery Departments at the University Hospital Joan XXIII (Tarragona, Spain) and University Hospital Virgen de la Victoria (Málaga, Spain) in accordance with the Declaration of Helsinki. Appropriate Institutional Review Board approval and biobank informed consent was obtained from all participants. Biobank samples included total and fractionated adipose tissue from subcutaneous and visceral origin, serum and plasma. All patients had fasted overnight before collection of blood and adipose tissue samples. Plasma and serum samples were stored at −80 °C prior to performing measurements. See Supplementary Experimental Procedures for further details.

2.10. Statistical analyses

Statistical analysis was performed with the Statistical Package for the Social Sciences software, version 15 (SPSS, Chicago, IL). For *in vitro* data, experimental results are presented as mean ± SEM from 3 to 4 independent experiments performed at least in duplicate. Statistical significance was tested with unpaired Student's t test or one-way ANOVA followed by the protected least-significant different test. For clinical and anthropometrical variables, normal distributed data are expressed as mean value ± SD, and for variables with no Gaussian distribution values are expressed as median (interquartile range). For analysis of expression variables that do not have a Gaussian distribution, values were analyzed by nonparametrical tests. Differences in clinical variables, laboratory parameters, or expression variables between groups were compared using ANOVA with *post hoc* Scheffe correction. Potential differences between depots were analyzed by nonparametric paired-samples test (Wilcoxon test). Interactions between factors as well as the effects of covariates and covariate interactions with factors were assessed by Pearson's correlation analysis and General Linear Model Univariate Analysis. Correction for confounding and interacting variables was performed using stepwise multiple linear regression analysis.

3. RESULTS

3.1. Hypoxia modulates extracellular glucose destination and promotes glycogen accumulation in human adipocytes

Hypoxia has been proposed as an important stimulus for aberrant adipose tissue inflammation and metabolism in obesity [24—26], and provides a good model system to study mechanisms of obesity-linked adipocyte dysfunction. It has been recently shown that hypoxia might influence glucose metabolism in adipocytes to prevent oxidative damage [27]. Similar to the findings in other cellular models of obesity-associated insulin resistance [28—31], we found that glucose uptake is increased in SGBS adipocytes subjected to hypoxia (Figure 1A). This increase in glucose uptake correlates with significantly greater mRNA expression of glucose transporters *GLUT1* and *GLUT4* and a non-significant increase in *GLUT3* expression (Figure 1B). To determine whether glucose metabolism was altered by hypoxia, we measured [^{13}C]-enrichment in human adipocytes incubated with uniformly labeled [U-^{13}C]-glucose or natural abundance glucose. Nuclear magnetic resonance (NMR) spectroscopy of lipid extracts from adipocytes cultured in hypoxia and normoxia revealed a similar incorporation of [^{13}C] into lipid structures (Normoxia: 1.29% ± 0.06 vs. Hypoxia: 1.20% ± 0.03). Also, no significant differences were detected in the relative total lipid content between the two conditions (Figure S1). However, mass spectrometry (MS) metabolic profiling of aqueous extracts from adipocytes subjected to hypoxia or normoxia unexpectedly revealed that intracellular levels of glucose, the glycolysis end product pyruvate, and the tricarboxylic acid (TCA) cycle intermediate succinate, were all significantly reduced in hypoxia-cultured cells (Figure 1C). Despite the differences in the pool size of these metabolites, the percentage of [^{13}C]-labeled metabolites arising from [U-^{13}C]-glucose did not differ between normoxia and hypoxia treatments (Figure S2). Given that high glucose uptake in hypoxia-cultured human adipocytes appeared not to be related to lipid biosynthesis or

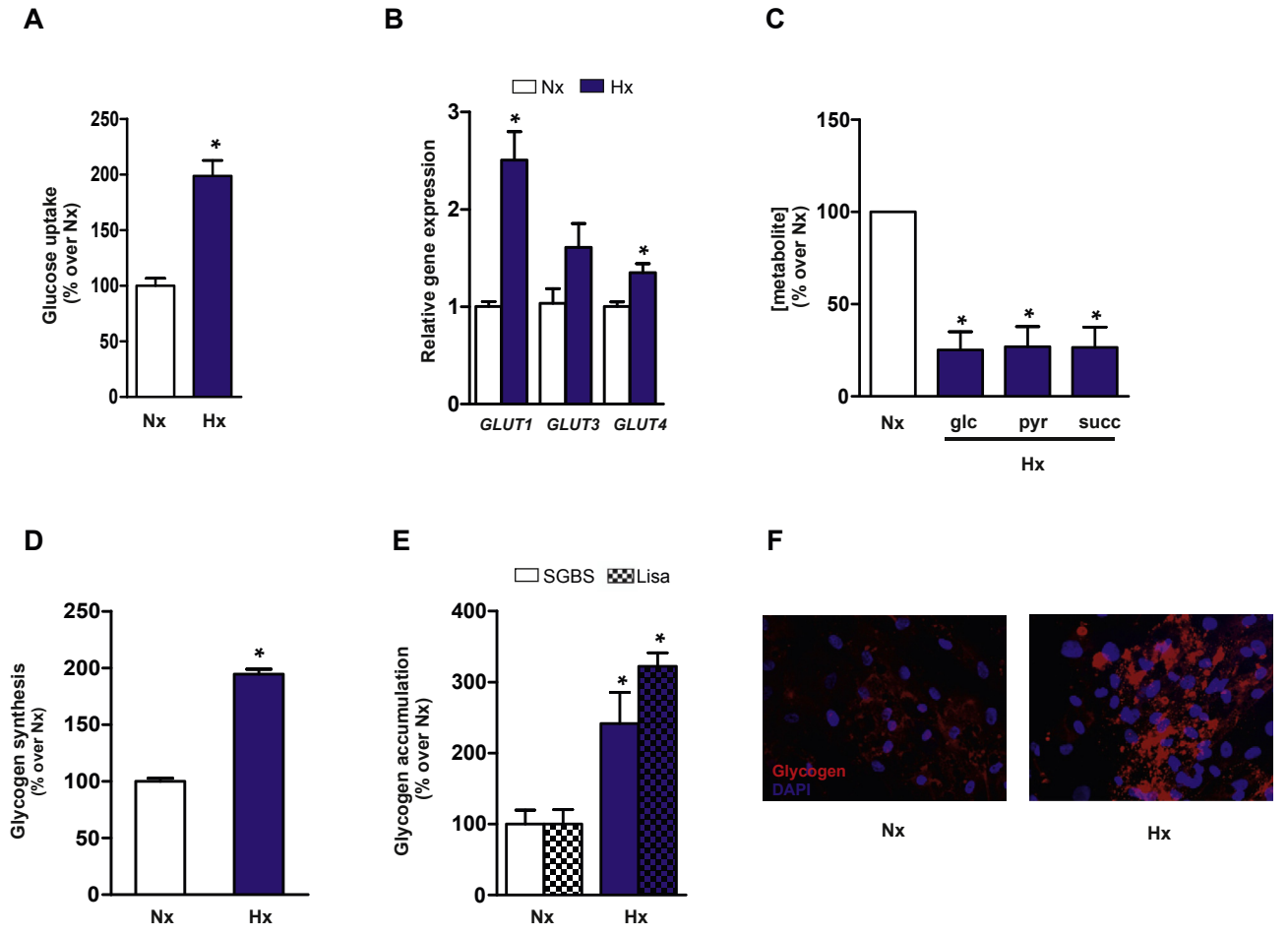

Figure 1: Hypoxia increases glucose uptake and promotes glycogen accumulation in human adipocytes. SGBS adipocytes were placed in hypoxia (Hx: 2% oxygen) or normoxia (Nx: 21% oxygen) for 24 h. (**A**) Basal glucose uptake measured during the last 10 min of incubation by quantification of 2-deoxyglucose incorporation. Results are mean ± SEM of 3 independent experiments performed in triplicate. *$p < 0.01$ vs Nx. (**B**) GLUT1, GLUT3 and GLUT4 mRNA expression analyzed by qPCR. Results are mean ± SEM of 3 independent experiments performed in duplicate and are expressed as relative expression to normoxic cells. *$p < 0.05$ vs. Nx. (**C**) Intracellular glucose, pyruvate and succinate levels were analyzed by MS. Results are mean ± SEM of 3 independent experiments performed in triplicate and are expressed as the percentage of metabolite levels over control cells. *$p < 0.01$ vs Nx. (**D**) Glycogen synthesis rate was analyzed in cells incubated with 20 mM [U-14C] glucose. *$p < 0.01$ vs. Nx. (**E**) Glycogen content in Lisa-2 and SGBS adipocytes incubated in Nx or Hx for 24 h. Results are mean ± SEM of 3 independent experiments performed in duplicate and are expressed as the percentage of stimulation over control cells. *$p < 0.05$ vs. Nx. (**F**) Immunofluorescent staining for glycogen in adipocytes obtained by differentiation of hASCs from lean subjects. Human mature adipocytes were incubated in Nx or Hx for 24 h. Nuclei were stained with DAPI (blue). Statistical significance was tested with unpaired Student's t test or one-way ANOVA followed by the protected least-significance different test.

TCA activity, we hypothesized that glucose metabolism might be redirected to glycogen synthesis. We therefore evaluated the impact of hypoxia on glycogen synthesis in adipocytes by measuring the rate of incorporation of radioactively labeled glucose into glycogen after a period of glucose deprivation. Hypoxia enhanced extracellular glucose deposition into glycogen (Figure 1D). Accordingly, analysis of glycogen content using the α-amyloglucosidase method revealed significant increases in intracellular glycogen in hypoxic SGBS and Lisa-2 adipocytes (Figure 1E). Increased glycogen content was also observed in hypoxia-cultured mature adipocytes obtained by differentiation of human adipose-derived stem cells (hASCs), as demonstrated by immunocytochemistry with a glycogen antibody (Figure 1F). Furthermore, intracellular levels of glycogen significantly decreased in SGBS and Lisa-2 adipocytes following 24 h of glucose deprivation, whereas stimulation with glucose and insulin increased glycogen accumulation (Figure S3). These data show that adipocytes can dynamically regulate their glycogen content in response to glucose availability and obesity-related stress conditions.

3.2. Glycogen deposition in adipocytes modifies their endocrine function via an autophagy-dependent mechanism

To examine whether glycogen accumulation might lead to metabolic changes in human adipocytes, we overexpressed the glycogen-targeting subunit PTG in SGBS cells by adenoviral infection. Analysis of glycogen levels (Figure 2A) and immunofluorescence staining with an antibody to glycogen (Figure 2B) demonstrated substantial glycogen deposition in PTG-expressing SGBS adipocytes but not in control (Ad-GFP) cells. Glycogen synthase protein levels were increased in Ad-PTG expressing cells, which correlated with a reduction in its inactive form (P-GS-Ser641) (Figure 2C). We also observed a decrease in glycogen phosphorylase (GP) protein expression in Ad-PTG expressing cells (Figure 2C). Thus, enforced expression of PTG increases glycogen synthesis and might inhibit glycogen degradation. Data from murine models reveal that enhancement of adipocyte glucose flux into glycogen exerts specific effects on the expression of leptin but not adiponectin [15]. To determine whether glycogen accumulation influenced the endocrine function of human adipocytes, we first analyzed

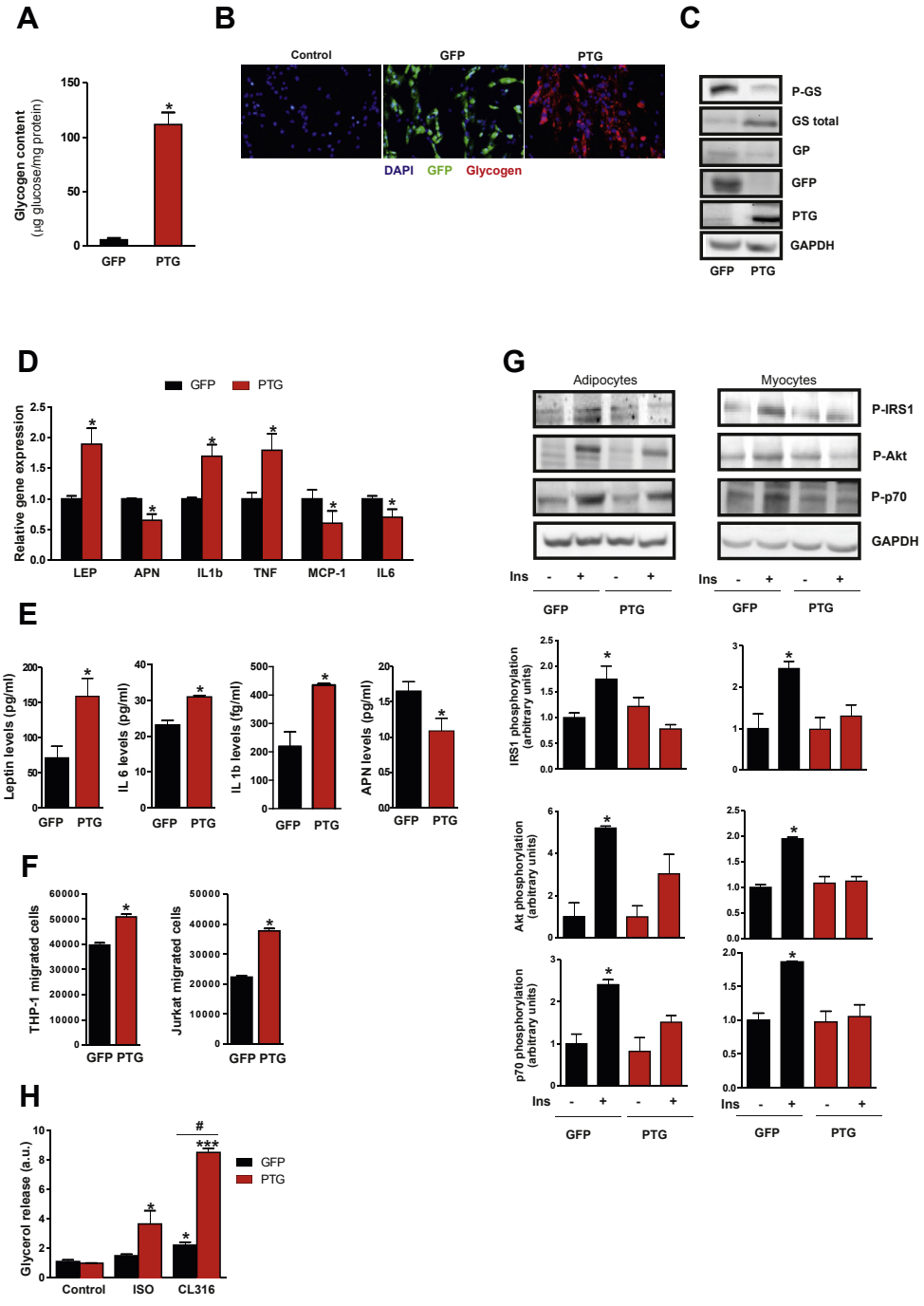

Figure 2: PTG overexpression in human adipocytes increases glycogen content and modulates adipocyte metabolism. Differentiated SGBS adipocytes were transduced with Ad- PTG or control Ad-GFP and analyzed 48 h post-infection. (**A**) Glycogen content. Results are mean ± SEM of 3 independent experiments performed in duplicate and are expressed as µg glucose/mg protein. *$p < 0.001$ vs. GFP. (**B**) Immunofluorescent staining for glycogen (red), GFP (green) and nuclei (blue). (**C**) Equal amounts of total cell extracts were subjected to immunoblotting with antibodies against total and phosphorylated GS (Ser641), GP, GFP and. PTG. GAPDH was used as a loading control. (**D**) Gene expression analysis of adipokines and inflammatory markers ($n = 4$). *$p < 0.05$ vs. GFP. (**E**) Leptin, IL-6, IL-1beta and adiponectin (APN) levels in the medium were analyzed by ELISA. *$p < 0.01$ vs. GFP. (**F**) Migration of THP-1 and Jurkat cells in response to conditioned medium from Ad-GFP or Ad-PTG-transduced SGBS adipocytes. *$p < 0.01$ vs. control cells. (**G**) Left Panel -Transduced cells were stimulated with 100 nM insulin for 15 min and total cell extracts were subjected to immunoblotting with antibodies against phosphorylated IRS1 (Tyr612), Akt (Ser473) and p70S6K (Thr421/Ser424). GAPDH was used as a loading control. Right panel- LHCNM2 myocytes were cultured for 24 h in conditioned medium from Ad-GFP- or Ad-PTG-transduced SGBS adipocytes, and were stimulated with 100 nM insulin for 15 min. Total cell extracts were subjected to immunoblotting with antibodies mentioned above. Quantification of 3 experiments is shown. *$p < 0.05$ vs. GFP cells. (**H**) Glycerol release was measured in Ad-GFP- and Ad-PTG-transduced cells in response to lipolytic stimulus (10 nM Isoproterenol and CL-316243). ($n = 3$). *$p < 0.05$; ***$p < 0.001$ vs. control cells. #$p < 0.05$ vs. GFP cells. Statistical significance was tested with unpaired Student's t test or one-way ANOVA followed by the protected least significance different test.

adipokine and cytokine gene expression in Ad-PTG transduced cells. Compared with control cells, mRNA expression of leptin, IL1-beta and TNF-alpha increased significantly upon PTG overexpression, whereas adiponectin, MCP-1 and IL-6 gene expression decreased significantly (Figure 2D). Among these genes, however, only leptin, IL-1beta and adiponectin showed a similar pattern of gene expression and protein secretion (Figure 2E). Consistent with the increase in leptin expression, conditioned medium from PTG-overexpressing cells (adip-CM) enhanced the migratory capacity of human monocytic THP-1 cells and Jurkat T cells (Figure 2F). To test whether these changes in endocrine function might also modulate insulin sensitivity, we next assessed insulin signaling in glycogen-loaded adipocytes. Insulin-induced phosphorylation of insulin receptor substrate-1 (IRS-1), Akt and p70S6K was significantly blunted in Ad-PTG-transduced adipocytes relative to equivalent Ad-GFP cells (Figure 2G). A similar result was obtained in human myocytes cultured for 24 h with adip-CM (Figure 2G). Basal adipocyte metabolism was unaffected by glycogen accumulation since similar cellular respiratory rates, metabolic gene expression and lactate release were observed in glycogen-loaded adipocytes and control cells (Figure S4). Nevertheless, an increase in the sensitivity to the lipolytic agents isoproterenol and CL-316243 was evident in glycogen-loaded adipocytes (Figure 2H), supporting the metabolic link proposed previously between lipid and carbohydrate metabolism [16,32].

We next sought to explore the potential mechanism(s) by which glycogen accumulation alters the endocrine function of adipocytes. In this context, increasing evidence from diverse model systems suggests a dynamic regulatory cross-talk between autophagy and glycogen metabolism [33]. Intriguingly, forced glycogen deposition in Ad-PTG-expressing human adipocytes led to an increase in autophagic flux as revealed by the increased expression of key autophagy-related proteins including GABARAPL1 and L3CBII (Figure 3A). No differences, however, were observed between Ad-PTG cells and Ad-GFP cells in the expression of starch-binding domain-containing protein 1 (STBD1), which has been directly related to autophagic degradation of glycogen particles with aberrant branching (termed glycophagy) [34,35]. Moreover, ER stress markers (GRP78, CHOP) and NF-κB signaling components (IκBα and IκBβ) were unchanged in PTG overexpressing cells (Figure 3A). Unexpectedly, this apparent activation of autophagy in glycogen-loaded adipocytes was associated with an inhibition of AMPK and mTORC1 signaling. Consequently, we detected a decrease in the expression of the active form of mTOR and phosphorylation of its downstream targets, p70S6K and ULK1, in Ad-PTG adipocytes relative to Ad-GFP cells (Figure 3B). Although no differences were detected in

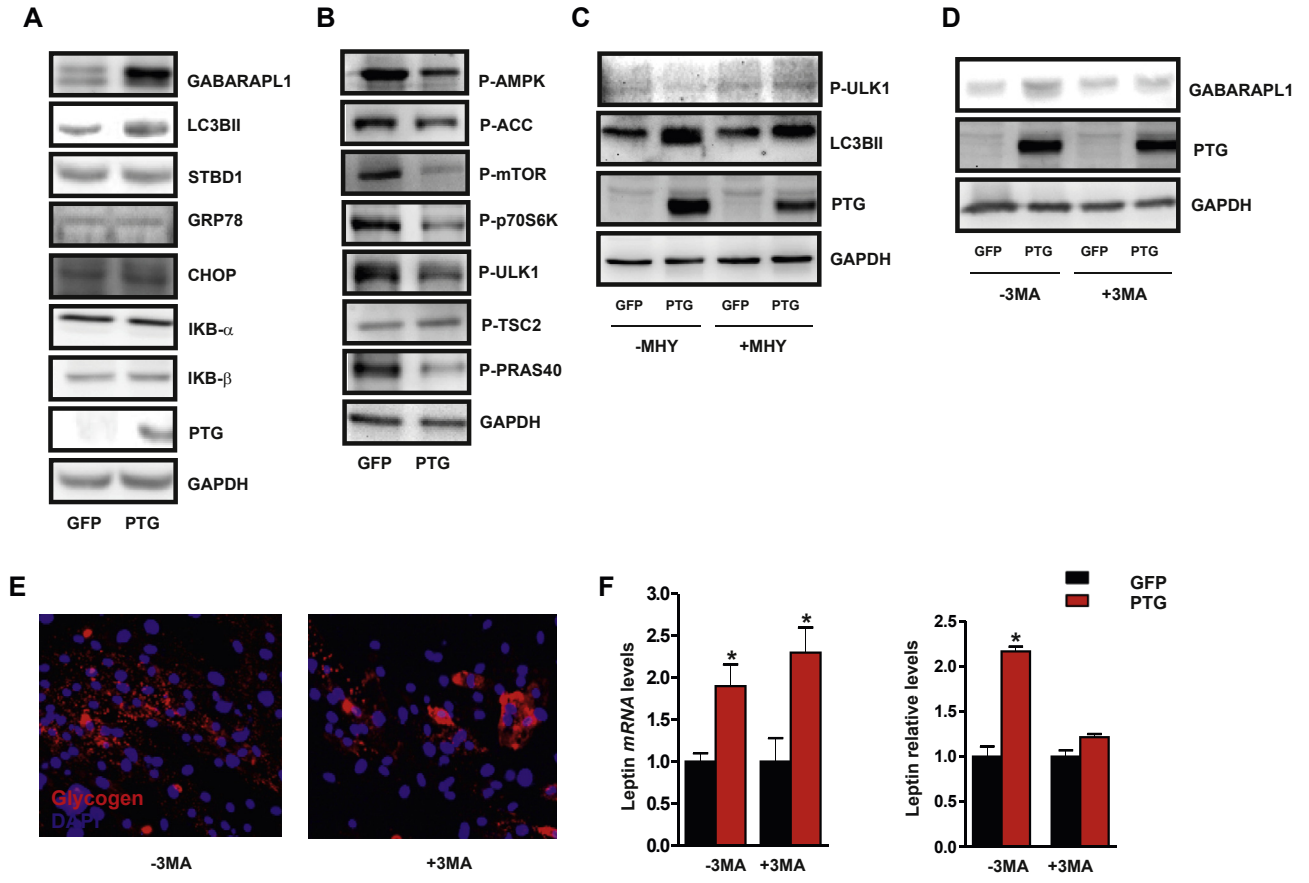

Figure 3: Enforced glycogen deposition in human adipocytes stimulates leptin secretion through an autophagy-dependent mechanism. Differentiated SGBS adipocytes ($n = 4–5$) were transduced with Ad-PTG or control Ad-GFP and analyzed 48 h post-infection. **(A–B)** Total cell extracts from transduced differentiated SGBS cells were subjected to immunoblotting with the indicated antibodies. GAPDH was used as a loading control. **(C)** Adipocytes were treated or not with 5 mM MHY1485. Total cell extracts were subjected to immunoblotting with antibodies against phosphorylated ULK1 (Ser758), L3CBII and PTG. GAPDH was used as a loading control. **(D)** Transduced SGBS adipocytes were treated or not with 5 mM 3-MA. Total cell extracts were subjected to immunoblotting with antibodies against GABARAPL1 and PTG. GAPDH was used as a loading control. **(E)** Immunofluorescence detection of glycogen (red). Nuclei were stained with DAPI (blue). **(F)** Leptin expression and secretion was analyzed by RT-qPCR and ELISA, respectively. *$p < 0.01$ vs. control cells. Statistical significance was tested with unpaired Student's t test followed by the protected least-significance different test.

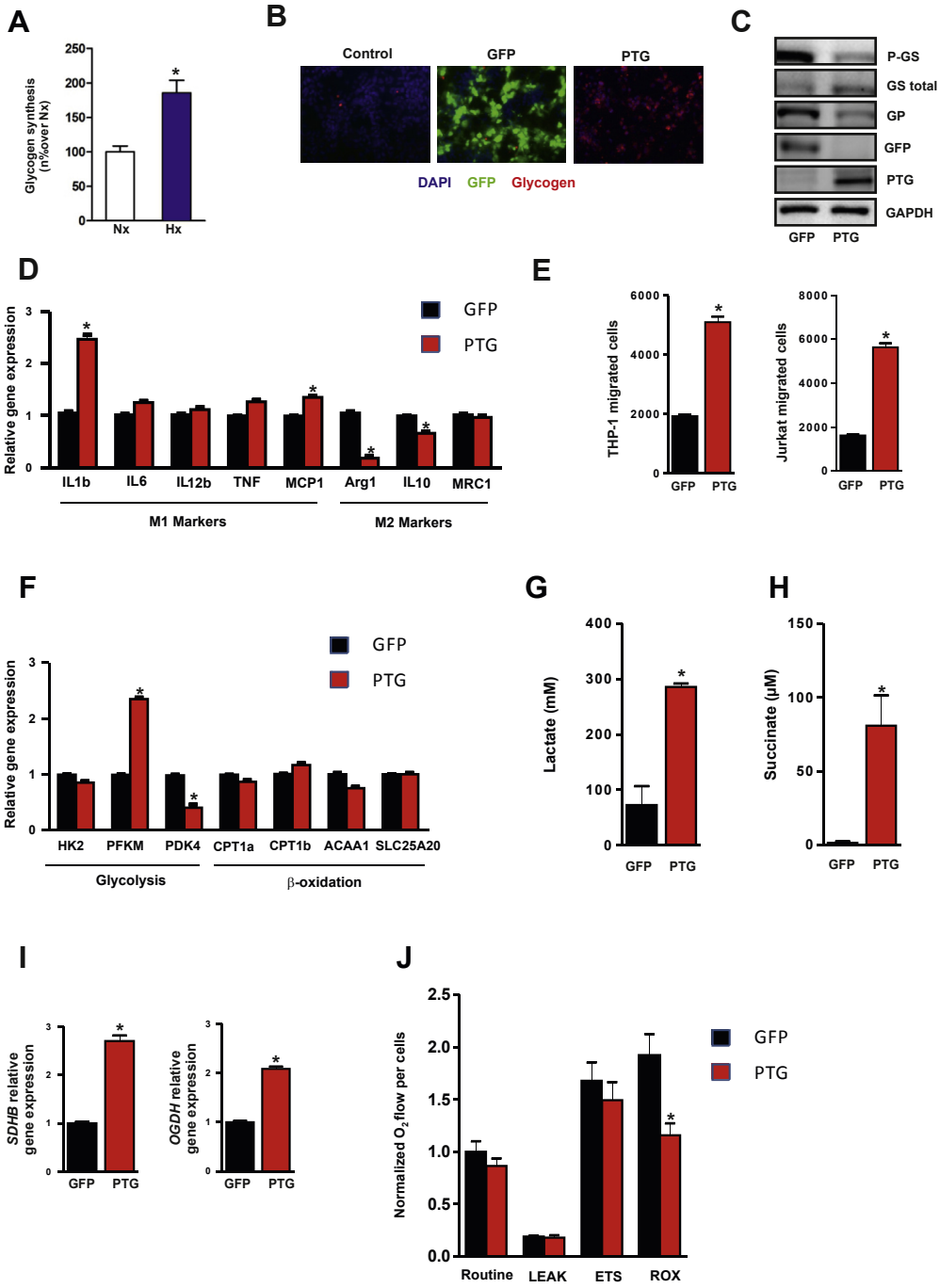

Figure 4: Enforced glycogen deposition in THP-1 macrophages stimulates a pro-inflammatory gene expression and glycolytic metabolic profile. Unactivated macrophages (M0) were transduced with Ad-PTG or control Ad-GFP and analyzed 48 h post-infection. **(A)** Glycogen synthesis. Results are mean ± SEM of 3 independent experiments performed in triplicate. *$p < 0.05$ vs. Nx. **(B)** Immunofluorescent staining for glycogen (red) and GFP (green) in THP-1 macrophages. Nuclei were stained with DAPI (blue). **(C)** Total cell extracts from transduced differentiated THP-1 cells were subjected to immunoblotting with the indicated antibodies. GAPDH was used as a loading control. **(D)** Expression of representative M1 and M2 marker genes in M0 infected macrophages. ($n = 3$) *$p < 0.05$ vs. GFP. **(E)** THP-1 and Jurkat cell migration using conditioned media of Ad- PTG or control Ad-GFP macrophages. ($n = 3$) *$p < 0.01$. **(F)** Metabolic gene expression profile of THP-1 macrophages infected with Ad-PTG or Ad- GFP. ($n = 3$) *$p < 0.05$. **(G)** Lactate and **(H)** Succinate accumulation in the conditioned medium of infected THP-1 macrophages. ($n = 3$) *$p < 0.01$. **(I)** Gene expression of representative TCA cycle genes in infected macrophages. ($n = 3$) *$p < 0.01$. **(J)** High-resolution respirometry studies were performed using an Oroboros-2kTM respirometer. Routine (basal), Leak respiration (uncoupled), ETS capacity (maximal) and ROX (non mitocondrial) values were measured. ($n = 4$) *$p < 0.05$. Statistical significance was tested with unpaired Student's t test or one-way ANOVA followed by the protected least-significance different test.

TSC2 phosphorylation at the Thr1462 residue, we observed a decrease in P-PRAS40 levels (Thr246), suggesting that mTORC1 regulation might be dependent on PRAS40 regulation (Figure 3B). We therefore used the mTOR activator MHY1485 [36] to question whether glycogen-induced autophagy is dependent on mTORC1 inhibition. The increase in mTOR-induced ULK1 phosphorylation at Ser758 detected in the presence of MHY1485 was associated with a decrease in L3CBII expression (Figure 3C). Finally, to examine a potential role for autophagy in the regulation of leptin production by glycogen accumulation, we utilized 3-methyladenine (3-MA) as a pharmacological inhibitor of autophagy [37]. Incubation of human adipocytes with 3-MA blocked the PTG-induced expression of GABARAPL1 (Figure 3D), but not glycogen accumulation (Figure 3E). Notably, 3-MA treatment had no effect on the PTG-induced increase in leptin gene expression but inhibited its secretion (Figure 3F), supporting the accumulating evidence that autophagy serves as a new mechanism to control protein trafficking and secretion [38]. Taken together, these results highlight the glycogen-autophagy intersection as a novel regulatory mechanism of leptin secretion in human adipocytes and suggest that modulation of glycogen levels in human adipocytes might modify their endocrine functions, contributing to adipose tissue inflammation and systemic insulin resistance.

3.3. Glycogen levels control the pro-inflammatory state of adipose tissue and promote macrophage M1 polarization

To study the *in vivo* function of PTG in adipose tissue inflammation, we first analyzed the inflammatory gene expression profile in adipose tissue from PTG KO mice and wild-type (WT) littermates [32]. Consistent with the link suggested between PTG overexpression and the pro-inflammatory state (Figure 2), PTG KO mice display reduced expression of several inflammatory gene markers in adipose tissue relative to WT mice (Figure S5). Differences in the expression of some of these genes (mainly MCP-1 and IL-6) between human cellular and murine models could be a consequence of comparing adipocytes (human cells) with whole adipose tissue (murine model). Because inflammatory responses in adipose tissue are dynamically regulated through innate immune cells, we further explored the effects of glycogen accumulation on the metabolic state and phenotype of human THP-1 macrophages. First, we confirmed that, similar to human adipocytes (Figure 1D), hypoxia enhanced extracellular glucose deposition in macrophages into glycogen (Figure 4A). Also, mirroring our observations in adipocytes (Figure 2B–C), PTG overexpression increased intracellular glycogen levels in THP-1 macrophages (Figure 4B), correlating with enhanced GS activity and decreased GP expression (Figure 4C). Since macrophages can adopt different activation states (classical M1 or alternative M2 activation) [39], we assessed whether enforced glycogen deposition influenced macrophage polarization. We analyzed M1 and M2 gene expression markers in Ad-PTG M0 (unactivated) macrophages and control cells (Ad-GFP M0). We observed an increase in the classical M1 markers IL-1β and MCP-1 in parallel with a decrease in the M2 markers Arg1 and IL-10 in glycogen-loaded M0 cells (Figure 4D). Moreover, monocyte and lymphocyte migration was increased with conditioned medium (CM) from PTG-overexpressing macrophages compared with CM from control cells (Figure 4E). More importantly, and consistent with published reports [40], we found that the commitment of glycogen-loaded M0 macrophages to the M1 phenotype was also evident in the metabolic gene expression profile, which was directed towards glycolysis (Figure 4F) and lactate release (Figure 4G). Furthermore, we detected an increase in the TCA cycle intermediate succinate, which has recently been associated with enhanced glycolysis and IL-1β secretion [41] (Figure 4H). Consistent with an increase in TCA activity, glycogen-loaded macrophages showed higher succinate dehydrogenase (SDHB) and alpha-ketoglutarate dehydrogenase (OGDH) gene expression (Figure 4I). Interestingly, although similar cellular respiratory rates were observed, a decrease in residual oxygen consumption (ROX) was detected in Ad-PTG macrophages compared with Ad-GFP macrophages, suggesting that the mitochondrial: non mitochondrial respiration ratio might be increased in Ad-PTG M0 macrophages (Figure 4J).

3.4. Altered expression of glycogen metabolic genes correlates with autophagy gene expression in human obesity

To determine whether obesity and insulin resistance altered glycogen metabolism in human adipose tissue, we analyzed several glycogen-related metabolic genes (Supplementary Experimental Procedures) in a well-characterized human cohort (clinical and laboratory data summarized in Table 1). We found a significant reduction in the expression of glucan (1,4-alpha) branching enzyme 1 (*GBE1*) and PP1-GTS 3E (*PPP1R3E*) mRNA in the subcutaneous adipose tissue (SAT) of obese subjects (Figure 5A). Bivariate analysis revealed that *GBE1* gene expression levels correlated negatively with body mass index (BMI),

Table 1 — Anthropometric and biochemical variables in the two cohorts studied for mRNA and protein expression levels.

	First cohort		Second cohort	
	Lean	Obese	Lean	Obese
N	19	37	10	38
Sex (male/female)	13/6	22/15	5/5	16/22
Age (years)	51.68 ± 15.96	58.58 ± 13.21	42.90 ± 10.70	41.97 ± 11.91
BMI (kg/m^2)	23.11 ± 1.59	29.07 ± 3.02[a]	23.29 ± 1.33	42.39 ± 14.57[a]
Waist (cm)	83.7 ± 7.9	99.29 ± 14.33[a]	83.15 ± 6.78	116.22 ± 25.5[a]
DBP (mmHg)	68.47 ± 9.90	76.4 ± 11.77[b]	78.80 ± 19.62	79.14 ± 12.98
SBP (mmHg)	121.47 ± 11.77	135.84 ± 16.90[b]	110.10 ± 21.94	131.11 ± 18.26[a]
Glucose (mmol/L)	4.33 ± 0.68	5.56 ± 0.49[a]	4.77 ± 0.63	5.19 ± 0.63
Cholesterol (mmol/L)	5.19 ± 1.18	5.10 ± 0.95	5.32 ± 1.06	5.12 ± 1.01
HDLc (mmol/L)	1.46 ± 0.21	1.35 ± 0.29	1.52 ± 0.39	1.26 ± 0.36
Triglycerides (mmol/L)	1.15 ± 0.53	1.17 ± 0.66	1.11 ± 0.58	1.45 ± 0.69
Insulin (μIU/ml)	4.52 ± 3.44	6.71 ± 4.94	6.75 ± 2.67	15.87 ± 11.56[a]
HOMA-IR	1.11 ± 0.84	1.74 ± 1.35	1.40 ± 0.48	3.81 ± 2.83[b]

The results are given as the mean ± SD. BMI: body mass index; DBP: Diastolic Blood Pressure; SBP: Systolic Blood Pressure. HOMA-IR: homeostasis model assessment of insulin resistance index. [a] indicate significant differences between the means of the different groups: a: $p < 0.001$: b: $p < 0.01$ (Student t test).

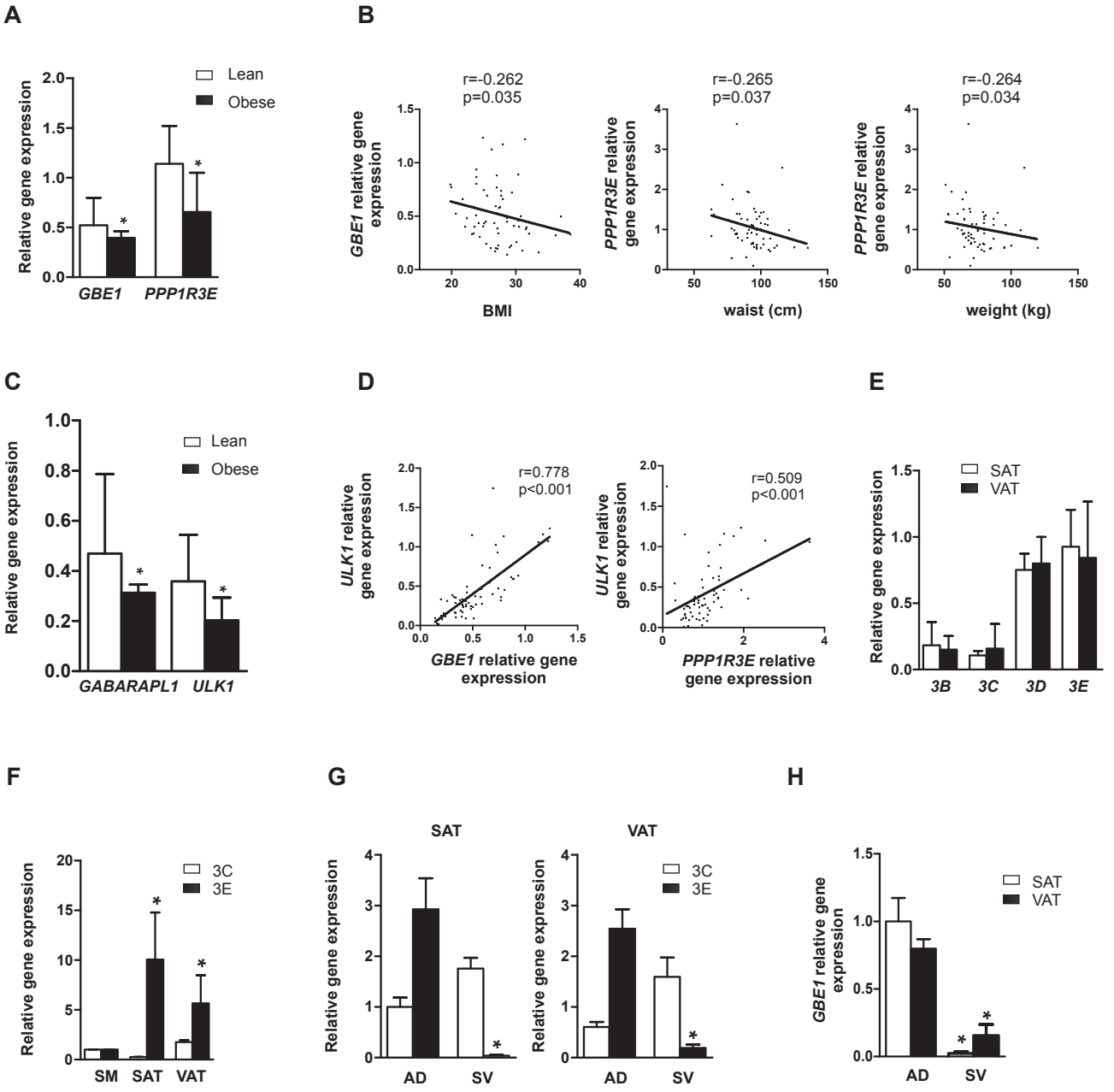

Figure 5: Human obesity is associated with changes in adipose glycogen metabolism and autophagy gene expression. (**A**) GBE1 and PPP1R3E mRNA expression in SAT depots of subjects from the first cohort (n = 56) divided into two groups according to BMI (lean: BMI<25 and obese: BMI>25). *p < 0.01 vs. lean. (**B**) Correlation between SAT GBE1 and PPP1R3E mRNA expression and clinical variables. (**C**) GABARAPL1 and ULK1 mRNA expression in SAT depots of subjects from the first cohort. (**D**) Bivariate correlations between glycogen metabolic genes (GBE1 and PPP1R3E) and ULK1. (**E**) PPP1R3B, PPP1R3C, PPP1R3D, PPP1R3E mRNA expression in SAT and VAT depots from the first cohort (n = 56). (**F**) PPP1R3C and PPP1R3E mRNA expression in SAT and VAT depots compared to skeletal muscle (SM) (n = 9) *p < 0.05. (**G**) PPP1R3C and PPP1R3E and (**H**) GBE1 mRNA expression in isolated adipocytes (AD) and stromal vascular fraction (SV) from SAT and VAT (n = 6; paired adipose biopsies). *p < 0.01. Data comparisons were made by Kruskal Wallis test for multiple groups and Mann Whitney test for two groups. Potential differences between depots were analyzed by nonparametric paired-samples test (Wilcoxon test). Interactions between factors as well as the effects of covariates and covariate interactions with factors were assessed by Pearson's correlation analysis and General Linear Model Univariate Analysis. Data are presented as median with interquartile range (A and C) and as mean ± SEM (E, F, G and H). *p < 0.01.

whereas *PPPR13E* was negatively associated with waist circumference and weight (Figure 5B). Given the relationship found between glycogen metabolism and autophagy *in vitro*, we analyzed the gene expression profile of autophagy-related genes in the same cohort (Supplementary Experimental Procedures). Interestingly, SAT depots from obese individuals exhibited lower mRNA levels of *GABARAPL1* and *ULK1* (Figure 5C). Additionally, consistent positive correlations were found between glycogen metabolic genes (*GBE1* and *PPP1R3E*) and *ULK1* mRNA expression (Figure 5D). More importantly, multiple regression analysis adjusting for age and gender revealed that *ULK1* predicts *GBE1* (B = 0.548; P < 0.001) and *PPP1R3E* (B = 0.649; P = 0.001) gene expression in SAT. To date, PTG (*PPP1R3C*) is the only reported PP1-GTS expressed in murine adipocytes (15). Of note, we found that *PPP1R3E* was the most predominant PP1-GTS isoform in human VAT

and SAT depots (Figure 5E). Indeed, *PPPR13E* mRNA is highly expressed in adipose tissue (VAT and SAT) relative to human skeletal muscle (Figure 5F), where a high level of this isoform was previously demonstrated [23]. In addition, we confirmed that *PPP1R3E* mRNA is found predominantly in mature adipocyte cells in human adipose tissue and not in other cells from the stromal-vascular (SV) pool (Figure 5G). Similarly, GBE1 is essentially restricted to mature adipocytes, with a lower signal in the SV fraction (Figure 5H). As a whole, our *in vivo* observations consolidate a significant association between glycogen metabolism and autophagy in human adipocytes.

3.5. Human obesity is associated with enhanced protein levels of GS and glycogen stores in adipose tissue

To validate our gene expression data, we performed protein expression studies in a selected number of subjects from a second independent cohort (clinical and laboratory data summarized in Table 1), in which circulating leptin levels were confirmed to be higher in obese subjects than in lean individuals (58.49 $\pm$ 7.10 vs. 19.96 $\pm$ 10.98 pg/ml). In agreement with mRNA levels, obese subjects presented a significant reduction in GBE1 and PPP1R3E protein expression in the SAT depot compared with lean subjects (Figure 6A). Although we found no significant differences in mRNA expression, obesity was also associated with greater levels of GS protein in SAT (Figure 6A). To explore a potential link between glycogen metabolism in adipose tissue and insulin sensitivity, obese subjects from the second cohort were classified according to their insulin resistance assessed by HOMA-IR. No significant differences were found in GBE1 protein expression between both groups (low IR vs. high IR); however, obese patients with high HOMA-IR values (>3.2) presented a significant decrease in PPP1R3E protein expression in SAT depots compared with patients with low

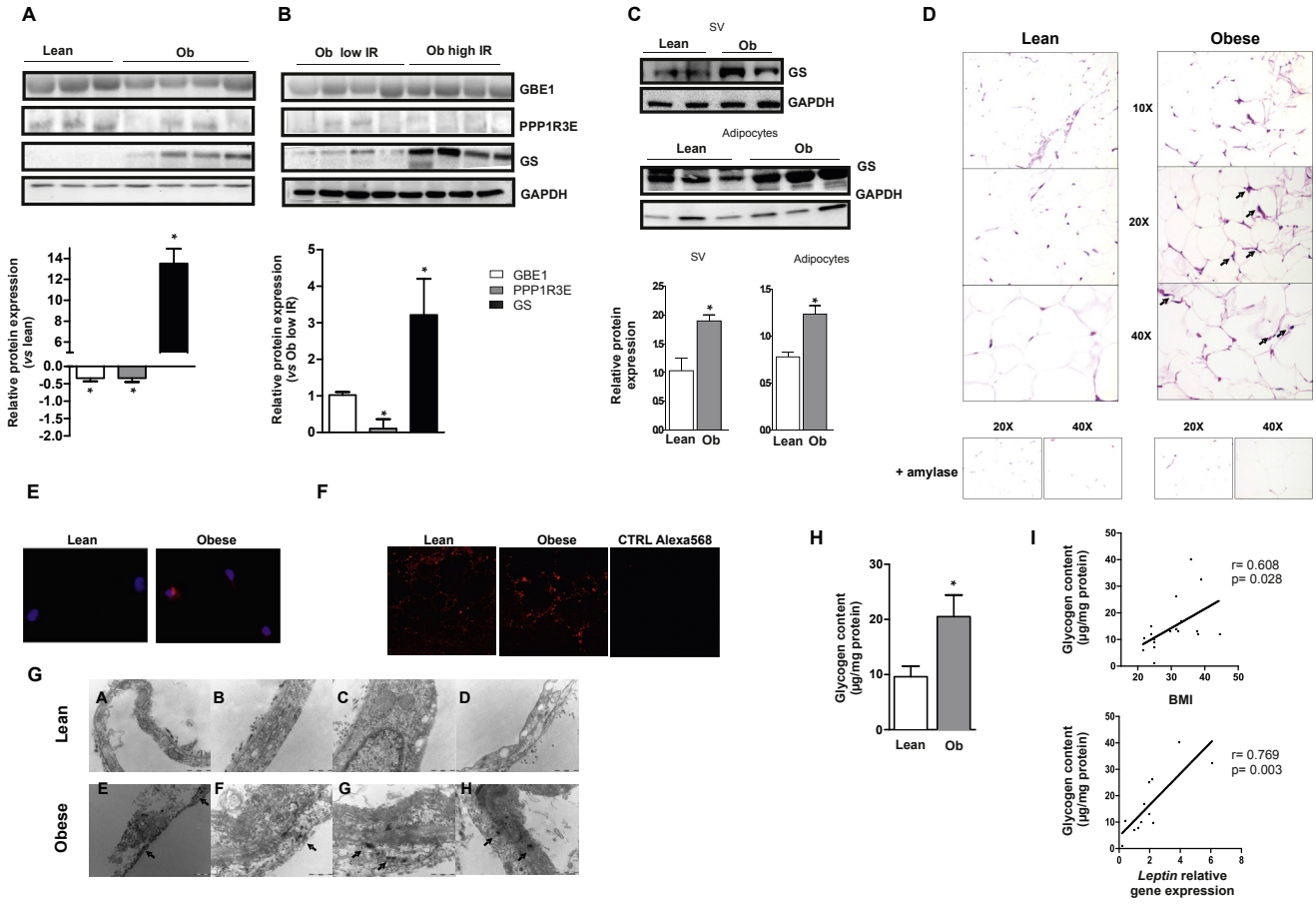

Figure 6: Human obesity leads to glycogen deposition in adipocytes. (**A**) Representative immunoblotting of GBE1, PPP1R3E and GS protein expression in SAT from subjects of the second cohort allocated into two groups according to BMI (lean: BMI<25, n = 5 and obese, Ob: BMI>25, n = 7). GAPDH was used as a loading control. Quantification is shown in the lower panels. *p < 0.05 vs. lean subjects. (**B**) Representative immunoblotting of GBE1, PPP1R3E and GS protein expression in SAT of obese subjects (Ob) classified according to insulin resistance assessed by HOMA-IR (low insulin resistance (low IR): HOMA-IR<3.2 and high insulin resistance (high IR): HOMA-IR>3.2). GAPDH was used as a loading control. Quantification is shown (n = 4). *p < 0.05 vs. obese low IR subjects. (**C**) Representative immunoblotting of GBE1 protein expression in isolated adipocytes (AD) and stromal vascular fraction (SV) from SAT depots of lean and obese patients. GAPDH was used as a loading control. Quantification is shown (n = 4). *p < 0.05 vs. lean subjects. (**D**) Representative histological analysis of SAT from lean and obese subjects using periodic acid-Schiff (PAS) staining for glycogen. Pretreatment with α-amylase eliminated PAS-positive staining in tissue sections, indicating specificity of staining for glycogen. Black arrows indicate macrophage-like structures. (**E**) Glycogen immunofluorescence (red) on macrophages extracted from lean or obese human adipose tissue. Nuclei were stained with DAPI (blue). (**F**) Representative glycogen immunofluorescent detection in SAT biopsies from lean and obese individuals. The negative control with the secondary antibody is also shown. ATMs (black arrows). (**G**) Glycogen detection in SAT from lean and obese subjects by transmission electron microscopy (TEM). Glycogen is visualized as small dark granules (black arrows). Representative images are shown (n = 6). (**H**) Glycogen content in mature adipocytes isolated from SAT of lean (n = 9) and obese (n = 10) subjects using α-amyloglucosidase method. Statistical significance was tested with unpaired Student's t test or one-way ANOVA followed by the protected least significance different test. (**I**) Bivariate correlations between glycogen content in mature adipocytes and BMI and Leptin mRNA expression (Pearson's correlation analysis).

values (HOMA-IR<3.2). Furthermore, we found significantly greater GS protein expression in the SAT depot of those insulin-resistant subjects (Figure 6B). Nevertheless, we found no differences in GS protein expression in lean subjects stratified as low/high IR (Figure S6), suggesting that alterations in GS might be related more to adiposity than to insulin resistance status. Importantly, the significant increase in GS protein expression was detected both in adipocytes and SV cells from SAT of obese subjects (Figure 6C). Further, we used different methodological approaches to assess whether human obesity could be related to changes in fat glycogen storage. Periodic acid-Schiff (PAS) staining of glycogen in SAT depots revealed an increase in total cellular glycogen in obese subjects, both in adipocytes and ATMs (Figure 6D). Immunofluorescent staining of glycogen in isolated macrophages from lean and obese subjects (Figure 6E), as well as in SAT depots (Figure 6F), confirmed these findings. Moreover, transmission electron microscopy (TEM) of fat tissue from biopsy specimens demonstrated that glycogen could be detected as small dark granules in the cytoplasm of subcutaneous adipocytes from obese patients (Figure 6G). Finally, we quantified glycogen content using the α-amyloglucosidase method in mature adipocytes isolated from SAT depots of lean and obese subjects. A significant increase of glycogen levels was detected in obese mature adipocytes (Figure 6H). Additionally, bivariate analysis revealed a positive association between glycogen content and BMI and also leptin expression (Figure 6I). Collectively, our results establish that adipose tissue glycogen deposition may underlie whole-body metabolic alterations found in human obesity.

4. DISCUSSION

Glucose is one of the major energy substrates for adipose tissue metabolism, and functional integrity of this organ in terms of glucose uptake is crucial for regulating intermediate metabolism [42,43]. Unlike skeletal muscle and liver, where glucose can be converted to glycogen (glycogenesis), it is thought that in adipose tissue, glucose is used mainly to provide energy or to supply glycerol phosphate for triacylglycerol synthesis [43]. Surprisingly, the potential role of glycogen metabolism in human adipose tissue and its effect on adipose tissue dynamics has received little attention.

Adipose tissue expansion in response to positive energy balance can lead to a myriad of local effects, including hypoxia [44]. Here we demonstrate that a redirection of glucose flux to glycogen synthesis occurs as a response to hypoxia in human adipocytes and macrophages, and we provide evidence that glycogen accumulation results in a damaging metabolic and secretory profile in these cells. We postulate that the increase of basal glucose uptake observed in obesity-linked conditions, such as hypoxia (this study) [45], hyperinsulinemia [28], pro-inflammatory cytokine activation [46,47] or endoplasmic reticulum stress [48], might be associated with a redirection of glucose metabolism to glycogenesis.

Our study provides insights into the metabolic consequences of glycogen overcapacity in human adipose tissue. Adipocyte glycogen accumulation provokes damaging effects as previously demonstrated in several cell types including neurons and retinal pigment epithelium [49–51]. Thus, enforced glycogen deposition modifies the adipocyte secretion pattern to one that is characterized by a decrease in the anti-inflammatory adipokine adiponectin and an increase in leptin secretion, in agreement with previous findings in PTG-transgenic mice [15]. Leptin is a potent chemoattractant for monocytes, neutrophils and dendritic cells [52–55], and also activates the expression of other pro-inflammatory cytokines [54]. Consequently, deleterious effects in terms of insulin sensitivity and immune cell recruitment were detected in PTG-expressing adipocytes. Contrary to the *in vivo* data from aP2-PTG transgenic mice [16], we observed higher rates of lipolysis in glycogen-loaded adipocytes, which, combined with their altered secretory profile, might contribute to the insulin resistant state associated with obesity. Critically, glycogen accumulation has a pro-inflammatory effect in macrophages. Accordingly, enforced glycogen deposition in inactive macrophages increases pro-inflammatory gene expression, glycolysis and succinate release, reflective of an M1 phenotype as previously described [41]. Together, our data identifies glycogen as an inflammatory metabolic signal in adipose tissue.

Of note, we report for the first time a new regulatory glycogen-autophagy crosstalk mechanism controlling leptin secretion in human adipocytes, which bolsters emerging discoveries linking autophagy to biosynthetic processes [32] and cytokine release [56]. Generally activated by nutrient deprivation, autophagy flux in glycogen-loaded adipocytes correlates with a negative regulation of the nutrient-sensing kinase mTOR, which has been previously associated with autophagy activation [57], but not with ER stress or NFKβ signaling, as detected in other cellular systems [58,59]. In fact, inhibition of mTORC1 is sufficient to induce autophagy in the presence of nutrients [60]. Unexpectedly, glycogen-loaded adipocytes did not display differences in TSC2 phosphorylation, but a decrease in P-PRAS40 (Thr246), an upstream negative regulator of mTORC1 [61], was observed suggesting that mTORC1 regulation in our model might be produced in a TSC2-independent, PRAS40-dependent, manner. PRAS40 phosphorylation could be AKT-dependent or −independent [62], and additional studies are needed to elucidate the mechanism by which glycogen accumulation controls mTORC1 activity. Remarkably, the presence of a glycogen sensor in the mTOR pathway has also been recently suggested in liver, where glycogen has been revealed as an important coordinator of glucose and lipid metabolism [32].

It is also noteworthy that although AMPK-mTOR-Ulk1/2 metabolic cross-talk is considered an important regulator of autophagy [63], we found that the accumulation of glycogen in human adipocytes and subsequently autophagy activation is associated with mTORC1 but also AMPK inactivation. However, the glycogen-binding domain on the AMPKβ subunit has been revealed as a regulatory domain that inhibits AMPK phosphorylation by upstream kinases [64] and Ulk1 might also directly phosphorylates and inactivates AMPK [65]. Accordingly, it is not unreasonable to suggest a model where adipocytes may sense pathological accumulation of glycogen through an mTORC1 mechanism independent of AMPK. The fact that adipocytes from an obese context behave as if they are in a nutrient and energy deprivation state suggests a disturbance in some cellular energetic sensor and point to mTORC1 signaling as a key regulator of adipocyte metabolism in pathological conditions.

Intriguingly, the proposed networking of glycogen with autophagy is also observed in human adipose tissue with implications for obesity. Interestingly, and contrary to murine models [15], our data establish *PPP1R3E* as the major PP1-GST isoform expressed in human adipocytes, and PTG (*PPP1R3C*) is mainly found in the SV fraction. Similar to PTG, *PPP1R3E* overexpression results in glycogen accumulation in SGBS adipocytes (Figure S7). Obese subjects display an obvious increase in glycogen deposition in adipocytes, which correlates with a decrease in GBE1 and PPP1R3E, but more importantly with an increase of GS protein expression. Indeed, obese patients with the highest degree of insulin resistance present the highest protein levels of GS. Remarkably, glycogen content in mature adipocytes positively correlates with BMI and leptin expression, supporting the link found *in vitro* between adipocyte glycogen and leptin. The reduced levels of some glycogen metabolic genes detected in obese adipose tissue may

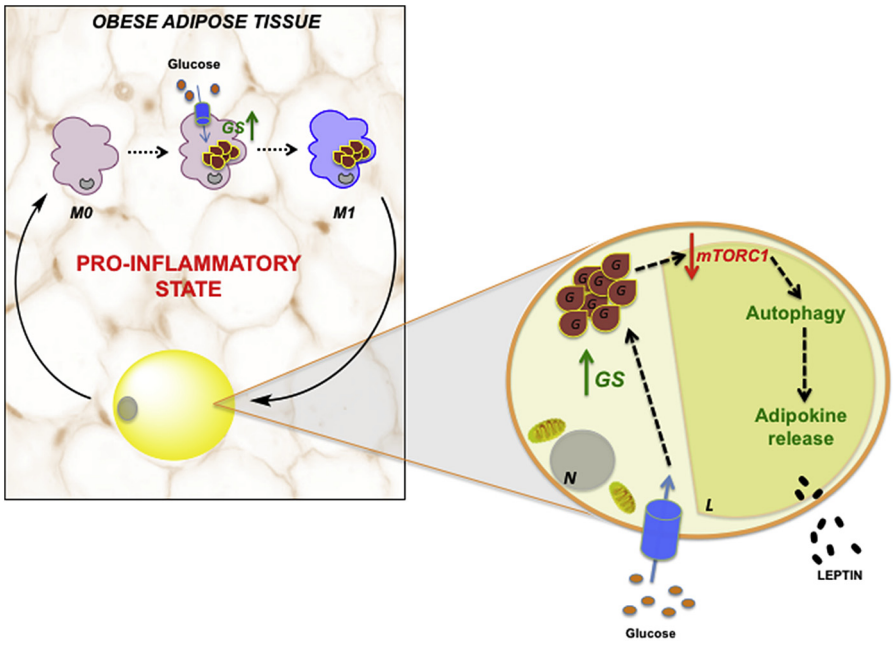

Figure 7: Adipose tissue glycogen accumulation as a potential trigger of obesity-linked inflammation in humans. In the context of human obesity, adipocytes and ATMs exhibit a redirection in glucose metabolism to glycogen synthesis (glycogenesis). Glycogen-loaded adipocytes present an increased autophagic flux, which, in turn, directly impacts their secretory function, encouraging immune cell recruitment and insulin resistance. Additionally, glycogen deposits in inactivated (M0) macrophages promotes M1 polarization, suggesting that adipose tissue glycogen might be a metabolic inflammatory signal in human obesity. **L** = lipid droplet; **N** = nucleus; **G** = glycogen accumulation; **GS** = glycogen synthase.

represent the onset of a counter regulatory mechanism as a defense against the pathological accumulation of glycogen in adipocytes. On the other hand, the correlation observed between several markers of glycogen synthesis and autophagy supports the link between both processes. Thus, *ULK1* was revealed as one of the main determinants of *GBE1* and *PPP1R3E* mRNA expression in SAT depots and was downregulated in obese subjects. We hypothesize that the reduction in *GABARAPL1* and *ULK1* gene expression detected in our cohorts might represent a compensatory mechanism for autophagy induction described in obese and diabetic patients [66–69].

In conclusion, this study provides the first evidence of adipose tissue glycogen as an inflammatory signal, which might underlie the pathogenesis of obesity and insulin resistance. We postulate that in an obesity setting, a shift from glycolytic metabolism to glycogenesis occurs in adipose tissue, which directly determines the secretory function of adipocytes by a mechanism dependent on autophagy flux activation, as well as an increase in the M1 polarized macrophage population (Figure 7). Whether glycogen mishandling is a primary disturbance or an indirect consequence of obesity is difficult to establish at the present time and awaits further investigation. Nonetheless, our study suggests metabolic disturbance in adipocytes as a potential primary event in obesity-related inflammation that should be considered in the development of new therapeutic strategies to alleviate obesity-associated metabolic disorders.

AUTHOR CONTRIBUTION

VCM, ME, CS, XD, MMG, KR, CNR and PP carried out the experiments and generated data. OY and MAR carried out the metabolomics studies. LGS and FT carried out part of the study selection and human sample processing. AGF, ES, PMG-R and ARS contributed to discussion and reviewed the manuscript. JV and SFV conceived the study, discussed data, and wrote the manuscript. JV and SFV are the guarantors of this work and, as such, had full access to all the data in the study and take responsibility for the integrity of the data and the accuracy of the data analysis.

ACKNOWLEDGMENTS

This study was supported by grants from the Spanish Ministry of Economy and Competitiveness (SAF2012-36186 to SF-V, PI14/00228 to JV and PI12/02355 to FJT). The Spanish Biomedical Research Center in Diabetes and Associated Metabolic Disorders (CIBERDEM) (CB07708/0012) is an initiative of the Instituto de Salud Carlos III. SF-V and LG-S acknowledge support from the "Miguel Servet" tenure-track program (CP10/00438 and CP13/00188, respectively) from the Fondo de Investigación Sanitaria (FIS) co-financed by the European Regional Development Fund (ERDF). We thank Dr. Maria Vinaixa and Sara Samino from Metabolomics Platform of CIBERDEM for their help with metabolomic analysis data, Pau Gama for their help with respirometry experiments and Dr. Kenneth McCreath for helpful comments on the manuscript. We also thank Dr. Otto Baba for his generous gift of the monoclonal glycogen antibody.

CONFLICT OF INTEREST

The authors have declared that no conflict of interest exists.

APPENDIX A. SUPPLEMENTARY DATA

Supplementary data related to this article can be found at http://dx.doi.org/10.1016/j.molmet.2015.10.001.

REFERENCES

[1] Krahmer, N., Farese Jr., R.V., Walther, T.C., 2013. Balancing the fat: lipid droplets and human disease. EMBO Molecular Medicine 5:905–915.

[2] Wu, H., Ballantyne, C.M., 2014. Inflammation versus host defense in obesity. Cell Metabolism 20:708–709.
[3] Beck-Nielsen, H., 2012. The role of glycogen synthase in the development of hyperglycemia in type 2 diabetes: 'To store or not to store glucose, that's the question'. Diabetes Metabolism Research and Reviews 28:635–644.
[4] Samuel, V.T., Petersen, K.F., Shulman, G.I., 2010. Lipid-induced insulin resistance: unravelling the mechanism. Lancet 375:2267–2277.
[5] Shulman, G.I., Rothman, D.L., Jue, T., Stein, P., DeFronzo, R.A., Shulman, R.G., 1990. Quantitation of muscle glycogen synthesis in normal subjects and subjects with non-insulin-dependent diabetes by 13C nuclear magnetic resonance spectroscopy. The New England Journal of Medicine 322: 223–228.
[6] Van Steenbergen, W., Lanckmans, S., 1995. Liver disturbances in obesity and diabetes mellitus. International Journal of Obesity and Related Metabolic Disorders 19(Suppl 3):S27–S36.
[7] Velho, G., Petersen, K.F., Perseghin, G., Hwang, J.H., Rothman, D.L., Pueyo, M.E., et al., 1996. Impaired hepatic glycogen synthesis in glucokinase-deficient (MODY-2) subjects. Journal of Clinical Investigation 98:1755–1761.
[8] Jensen, J., Lai, Y.C., 2009. Regulation of muscle glycogen synthase phosphorylation and kinetic properties by insulin, exercise, adrenaline and role in insulin resistance. Archives of Physiology and Biochemistry 115:13–21.
[9] Brady, M.J., Saltiel, A.R., 2001. The role of protein phosphatase-1 in insulin action. Recent Progress in Hormone Research 56:157–173.
[10] Montori-Grau, M., Guitart, M., Garcia-Martinez, C., Orozco, A., Gomez-Foix, A.M., 2011. Differential pattern of glycogen accumulation after protein phosphatase 1 glycogen-targeting subunit PPP1R6 overexpression, compared to PPP1R3C and PPP1R3A, in skeletal muscle cells. BMC Biochemistry 12:57.
[11] Newgard, C.B., Brady, M.J., O'Doherty, R.M., Saltiel, A.R., 2000. Organizing glucose disposal: emerging roles of the glycogen targeting subunits of protein phosphatase-1. Diabetes 49:1967–1977.
[12] Crosson, S.M., Khan, A., Printen, J., Pessin, J.E., Saltiel, A.R., 2003. PTG gene deletion causes impaired glycogen synthesis and developmental insulin resistance. Journal of Clinical Investigation 111:1423–1432.
[13] Rahman, S.M., Dobrzyn, A., Lee, S.H., Dobrzyn, P., Miyazaki, M., Ntambi, J.M., 2005. Stearoyl-CoA desaturase 1 deficiency increases insulin signaling and glycogen accumulation in brown adipose tissue. American Journal of Physiology, Endocrinology and Metabolism 288:E381–E387.
[14] Printen, J.A., Brady, M.J., Saltiel, A.R., 1997. PTG, a protein phosphatase 1-binding protein with a role in glycogen metabolism. Science 275:1475–1478.
[15] Jurczak, M.J., Danos, A.M., Rehrmann, V.R., Allison, M.B., Greenberg, C.C., Brady, M.J., 2007. Transgenic overexpression of protein targeting to glycogen markedly increases adipocytic glycogen storage in mice. American Journal of Physiology, Endocrinology and Metabolism 292:E952–E963.
[16] Markan, K.R., Jurczak, M.J., Allison, M.B., Ye, H., Sutanto, M.M., Cohen, R.N., et al., 2010. Enhanced glycogen metabolism in adipose tissue decreases triglyceride mobilization. American Journal of Physiology, Endocrinology and Metabolism 299:E117–E125.
[17] Vendrell, J., Maymo-Masip, E., Tinahones, F., Garcia-Espana, A., Megia, A., Caubet, E., et al., 2010. Tumor necrosis-like weak inducer of apoptosis as a proinflammatory cytokine in human adipocyte cells: up-regulation in severe obesity is mediated by inflammation but not hypoxia. Journal of Clinical Endocrinology & Metabolism 95:2983–2992.
[18] Serena, C., Calvo, E., Clares, M.P., Diaz, M.L., Chicote, J.U., Beltran-Debon, R., et al., 2015. Significant in vivo anti-inflammatory activity of Pytren4Q-Mn a superoxide dismutase 2 (SOD2) mimetic scorpiand-like Mn (II) complex. PLoS One 10:e0119102.
[19] Pachon-Pena, G., Yu, G., Tucker, A., Wu, X., Vendrell, J., Bunnell, B.A., et al., 2011. Stromal stem cells from adipose tissue and bone marrow of age-matched female donors display distinct immunophenotypic profiles. Journal of Cellular Physiology 226:843–851.
[20] Titos, E., Rius, B., Gonzalez-Periz, A., Lopez-Vicario, C., Moran-Salvador, E., Martinez-Clemente, M., et al., 2011. Resolvin D1 and its precursor docosahexaenoic acid promote resolution of adipose tissue inflammation by eliciting macrophage polarization toward an M2-like phenotype. Journal of Immunology 187:5408–5418.
[21] Gasa, R., Jensen, P.B., Berman, H.K., Brady, M.J., DePaoli-Roach, A.A., Newgard, C.B., 2000. Distinctive regulatory and metabolic properties of glycogen-targeting subunits of protein phosphatase-1 (PTG, GL, GM/RGI) expressed in hepatocytes. Journal of Biological Chemistry 275:26396–26403.
[22] Burns, J., Neame, P.B., 1966. Staining of blood cells with periodic acid/salicyloyl hydrazide (PA-SH). A fluorescent method for demonstrating glycogen. Blood 28:674–682.
[23] Munro, S., Ceulemans, H., Bollen, M., Diplexcito, J., Cohen, P.T., 2005. A novel glycogen-targeting subunit of protein phosphatase 1 that is regulated by insulin and shows differential tissue distribution in humans and rodents. FEBS Journal 272:1478–1489.
[24] O'Rourke, R.W., White, A.E., Metcalf, M.D., Olivas, A.S., Mitra, P., Larison, W.G., et al., 2011. Hypoxia-induced inflammatory cytokine secretion in human adipose tissue stromovascular cells. Diabetologia 54:1480–1490.
[25] Trayhurn, P., Wang, B., Wood, I.S., 2008. Hypoxia and the endocrine and signalling role of white adipose tissue. Archives of Physiology and Biochemistry 114:267–276.
[26] Ye, J., 2009. Emerging role of adipose tissue hypoxia in obesity and insulin resistance. International Journal of Obesity (London) 33:54–66.
[27] Leiherer, A., Geiger, K., Muendlein, A., Drexel, H., 2014. Hypoxia induces a HIF-1alpha dependent signaling cascade to make a complex metabolic switch in SGBS-adipocytes. Molecular and Cellular Endocrinology 383:21–31.
[28] Fernandez-Veledo, S., Nieto-Vazquez, I., de Castro, J., Ramos, M.P., Bruderlein, S., Moller, P., et al., 2008. Hyperinsulinemia induces insulin resistance on glucose and lipid metabolism in a human adipocytic cell line: paracrine interaction with myocytes. Journal of Clinical Endocrinology & Metabolism 93:2866–2876.
[29] Fernandez-Veledo, S., Nieto-Vazquez, I., Vila-Bedmar, R., Garcia-Guerra, L., Alonso-Chamorro, M., Lorenzo, M., 2009. Molecular mechanisms involved in obesity-associated insulin resistance: therapeutical approach. Archives of Physiology and Biochemistry 115:227–239.
[30] Ranganathan, S., Davidson, M.B., 1996. Effect of tumor necrosis factor-alpha on basal and insulin-stimulated glucose transport in cultured muscle and fat cells. Metabolism 45:1089–1094.
[31] Terai, K., Hiramoto, Y., Masaki, M., Sugiyama, S., Kuroda, T., Hori, M., et al., 2005. AMP-activated protein kinase protects cardiomyocytes against hypoxic injury through attenuation of endoplasmic reticulum stress. Molecular and Cellular Biology 25:9554–9575.
[32] Lu, B., Bridges, D., Yang, Y., Fisher, K., Cheng, A., Chang, L., et al., 2014. Metabolic crosstalk: molecular links between glycogen and lipid metabolism in obesity. Diabetes 63:2935–2948.
[33] Singh, P.K., Singh, S., 2015. Changing shapes of glycogen-autophagy nexus in neurons: perspective from a rare epilepsy. Frontiers in Neurology 6:14.
[34] Jiang, S., Heller, B., Tagliabracci, V.S., Zhai, L., Irimia, J.M., DePaoli-Roach, et al., 2010. Starch binding domain-containing protein 1/genethonin 1 is a novel participant in glycogen metabolism. Journal of Biological Chemistry 285: 34960–34971.
[35] Jiang, S., Wells, C.D., Roach, P.J., 2011. Starch-binding domain-containing protein 1 (Stbd1) and glycogen metabolism: identification of the Atg8 family interacting motif (AIM) in Stbd1 required for interaction with GABARAPL1. Biochemical and Biophysical Research Communications 413:420–425.
[36] Choi, Y.J., Park, Y.J., Park, J.Y., Jeong, H.O., Kim, D.H., Ha, Y.M., et al., 2012. Inhibitory effect of mTOR activator MHY1485 on autophagy: suppression of lysosomal fusion. PLoS One 7:e43418.

[37] Caro, L.H., Plomp, P.J., Wolvetang, E.J., Kerkhof, C., Meijer, A.J., 1988. 3-Methyladenine, an inhibitor of autophagy, has multiple effects on metabolism. European Journal of Biochemistry 175:325–329.
[38] Deretic, V., Jiang, S., Dupont, N., 2012. Autophagy intersections with conventional and unconventional secretion in tissue development, remodeling and inflammation. Trends in Cell Biology 22:397–406.
[39] Lumeng, C.N., Saltiel, A.R., 2011. Inflammatory links between obesity and metabolic disease. Journal of Clinical Investigation 121:2111–2117.
[40] Zhu, L., Zhao, Q., Yang, T., Ding, W., Zhao, Y., 2015. Cellular metabolism and macrophage functional polarization. International Reviews of Immunology 34: 82–100.
[41] Mills, E., O'Neill, L.A., 2014. Succinate: a metabolic signal in inflammation. Trends in Cell Biology 24:313–320.
[42] Abel, E.D., Peroni, O., Kim, J.K., Kim, Y.B., Boss, O., Hadro, E., et al., 2001. Adipose-selective targeting of the GLUT4 gene impairs insulin action in muscle and liver. Nature 409:729–733.
[43] Leto, D., Saltiel, A.R., 2012. Regulation of glucose transport by insulin: traffic control of GLUT4. Nature Reviews Molecular Cell Biology 13:383–396.
[44] Trayhurn, P., 2013. Hypoxia and adipose tissue function and dysfunction in obesity. Physiological Reviews 93:1–21.
[45] Ceperuelo-Mallafre, V., Duran, X., Pachon, G., Roche, K., Garrido-Sanchez, L., Vilarrasa, N., et al., 2014. Disruption of GIP/GIPR axis in human adipose tissue is linked to obesity and insulin resistance. Journal of Clinical Endocrinology & Metabolism 99:E908–E919.
[46] Carey, A.L., Steinberg, G.R., Macaulay, S.L., Thomas, W.G., Holmes, A.G., Ramm, G., et al., 2006. Interleukin-6 increases insulin-stimulated glucose disposal in humans and glucose uptake and fatty acid oxidation in vitro via AMP-activated protein kinase. Diabetes 55:2688–2697.
[47] Fernandez-Veledo, S., Vila-Bedmar, R., Nieto-Vazquez, I., Lorenzo, M., 2009. c-Jun N-terminal kinase 1/2 activation by tumor necrosis factor-alpha induces insulin resistance in human visceral but not subcutaneous adipocytes: reversal by liver X receptor agonists. Journal of Clinical Endocrinology & Metabolism 94:3583–3593.
[48] Panzhinskiy, E., Ren, J., Nair, S., 2013. Protein tyrosine phosphatase 1B and insulin resistance: role of endoplasmic reticulum stress/reactive oxygen species/nuclear factor kappa B axis. PLoS One 8:e77228.
[49] Duran, J., Tevy, M.F., Garcia-Rocha, M., Calbo, J., Milan, M., Guinovart, J.J., 2012. Deleterious effects of neuronal accumulation of glycogen in flies and mice. EMBO Molecular Medicine 4:719–729.
[50] Hernandez, C., Garcia-Ramirez, M., Garcia-Rocha, M., Saez-Lopez, C., Valverde, A.M., Guinovart, J.J., et al., 2014. Glycogen storage in the human retinal pigment epithelium: a comparative study of diabetic and non-diabetic donors. Acta Diabetologica 51:543–552.
[51] Senanayake, P., Calabro, A., Hu, J.G., Bonilha, V.L., Darr, A., Bok, D., et al., 2006. Glucose utilization by the retinal pigment epithelium: evidence for rapid uptake and storage in glycogen, followed by glycogen utilization. Experimental Eye Research 83:235–246.
[52] Antuna-Puente, B., Feve, B., Fellahi, S., Bastard, J.P., 2008. Adipokines: the missing link between insulin resistance and obesity. Journal of Diabetes & Metabolism 34:2–11.
[53] Fantuzzi, G., 2006. Leptin: nourishment for the immune system. European Journal of Immunology 36:3101–3104.
[54] Schaffler, A., Scholmerich, J., Salzberger, B., 2007. Adipose tissue as an immunological organ: toll-like receptors, C1q/TNFs and CTRPs. Trends in Immunology 28:393–399.
[55] Zarkesh-Esfahani, H., Pockley, A.G., Wu, Z., Hellewell, P.G., Weetman, A.P., Ross, R.J., 2004. Leptin indirectly activates human neutrophils via induction of TNF-alpha. Journal of Immunology 172:1809–1814.
[56] Dupont, N., Jiang, S., Pilli, M., Ornatowski, W., Bhattacharya, D., Deretic, V., 2011. Autophagy-based unconventional secretory pathway for extracellular delivery of IL-1beta. EMBO Journal 30:4701–4711.
[57] Nazio, F., Strappazzon, F., Antonioli, M., Bielli, P., Cianfanelli, V., Bordi, M., et al., 2013. mTOR inhibits autophagy by controlling ULK1 ubiquitylation, self-association and function through AMBRA1 and TRAF6. Nature Cell Biology 15: 406–416.
[58] Kapuy, O., Vinod, P.K., Banhegyi, G., 2014. mTOR inhibition increases cell viability via autophagy induction during endoplasmic reticulum stress – an experimental and modeling study. FEBS Open Bio 4:704–713.
[59] Nikoletopoulou, V., Markaki, M., Palikaras, K., Tavernarakis, N., 2013. Crosstalk between apoptosis, necrosis and autophagy. Biochimica et Biophysica Acta 1833:3448–3459.
[60] Russell, R.C., Yuan, H.X., Guan, K.L., 2014. Autophagy regulation by nutrient signaling. Cell Research 24:42–57.
[61] Mi, W., Ye, Q., Liu, S., She, Q.B., 2015. AKT inhibition overcomes rapamycin resistance by enhancing the repressive function of PRAS40 on mTORC1/4E-BP1 axis. Oncotarget 6(16):13962–13977.
[62] Memmott, R.M., Dennis, P.A., 2009. Akt-dependent and -independent mechanisms of mTOR regulation in cancer. Cellular Signalling 21:656–664.
[63] Alers, S., Loffler, A.S., Wesselborg, S., Stork, B., 2012. Role of AMPK-mTOR-Ulk1/2 in the regulation of autophagy: cross talk, shortcuts, and feedbacks. Molecular and Cellular Biology 32:2–11.
[64] McBride, A., Ghilagaber, S., Nikolaev, A., Hardie, D.G., 2009. The glycogen-binding domain on the AMPK beta subunit allows the kinase to act as a glycogen sensor. Cell Metabolism 9:23–34.
[65] Loffler, A.S., Alers, S., Dieterle, A.M., Keppeler, H., Franz-Wachtel, M., Kundu, M., et al., 2011. Ulk1-mediated phosphorylation of AMPK constitutes a negative regulatory feedback loop. Autophagy 7:696–706.
[66] Jansen, H.J., van Essen, P., Koenen, T., Joosten, L.A., Netea, M.G., Tack, C.J., et al., 2012. Autophagy activity is up-regulated in adipose tissue of obese individuals and modulates proinflammatory cytokine expression. Endocrinology 153:5866–5874.
[67] Kovsan, J., Bluher, M., Tarnovscki, T., Kloting, N., Kirshtein, B., Madar, L., et al., 2011. Altered autophagy in human adipose tissues in obesity. Journal of Clinical Endocrinology & Metabolism 96:E268–E277.
[68] Nunez, C.E., Rodrigues, V.S., Gomes, F.S., Moura, R.F., Victorio, S.C., Bombassaro, B., et al., 2013. Defective regulation of adipose tissue autophagy in obesity. International Journal of Obesity (London) 37:1473–1480.
[69] Ost, A., Svensson, K., Ruishalme, I., Brannmark, C., Franck, N., Krook, H., et al., 2010. Attenuated mTOR signaling and enhanced autophagy in adipocytes from obese patients with type 2 diabetes. Molecular Medicine 16:235–246.

